Characterization of synthetic tridymites by transmission electron microscopy

Michael A. Carpenter

Department of Earth Sciences, University of Cambridge
Downing St., Cambridge CB2 3EQ, England

and Mechthild Wennemer

Institut für Kristallographie und Petrographie
E.T.H.–Zentrum, Zürich CH-8092, Switzerland

Abstract

Eight tridymites, synthesized in a variety of ways, have been examined by transmission electron microscopy (TEM). Each sample appeared to be heterogeneous, containing a mixture of low temperature structural forms. Two main structure types were identified: one with a pseudohexagonal superlattice, having $a = \sqrt{3}a_H$, $c = 2c_H$, and the second with a pseudo-orthorhombic C-face centered cell, having $a = 2\sqrt{3}a_H$, $b = 2a_H$ and with either a multiple c repeat or (001) stacking disorder (where a_H and c_H are respectively ~5Å, ~8.2Å and refer to the high temperature hexagonal sublattice). The former structure seemed to predominate in grains with few (001) stacking faults. In addition, some samples contained regions of considerable (001) disorder intergrown with more highly ordered material on a scale of a few hundred ångströms. Diffraction patterns from these grains could not be indexed easily on a known tridymite or cristobalite superlattice and have been tentatively ascribed to mixed (tridymite/cristobalite) layering.

High/low transformations were induced by beam heating. The $2\sqrt{3}a_H \times 2a_H \times nc_H$ type superstructures could be transformed reversibly to the hexagonal high temperature sublattice until radiation damage started to occur. In contrast, the $\sqrt{3}a_H \times 2c_H$ superlattice gave way to the high temperature hexagonal sublattice on heating but invariably reverted to a $2\sqrt{3}a_H \times 2a_H \times nc_H$ structure on subsequent cooling.

The diversity of superstructures observed in each sample helps to account for differences between the transformation behavior of many synthetic tridymite powders and larger natural or synthetic single crystals. In this context, TEM provides a useful adjunct to X-ray powder diffraction for the characterization of tridymites prepared for other types of experiments.

Introduction

It has long been known that tridymites undergo displacive structural transformations on heating and cooling. These transformations have been studied as functions of pressure and temperature by a variety of techniques, including optical microscopy with heating stages (Fenner, 1913; Flörke, 1955; Dollase et al., 1971; Nukui et al., 1978), single crystal or powder X-ray heating cameras (Gibbs, 1926; Buerger and Lukesh, 1942; Hill and Roy, 1958; Sato, 1963a, b, 1964; Dollase and Buerger, 1966; Tagai and Sadanaga, 1972; Kihara, 1977, 1978; Nukui et al., 1978; Hoffmann et al., 1983), the diamond anvil cell (Nukui et al., 1980), differential thermal analysis (Flörke, 1955; Flörke and Müller-Vonmoos, 1971; Cohen and Klement, 1980) and calorimetry (Mosesman and Pitzer, 1941; Shahid and Glasser, 1970; Thompson and Wennemer, 1979). One of the most striking features of the complex series of changes which have been observed is that different tridymites usually do not show the same sequence of structural changes

with the same transformation temperatures (reviewed by Flörke, 1955, 1967; Sosman, 1965; Nukui et al., 1978).

When tridymite samples used for transformation studies have been characterized by single crystal X-ray diffraction, the nature of each superstructure observed has been rather well defined (Dollase, 1967; Kihara, 1977; Nukui et al., 1978; Nukui et al., 1980; Hoffmann et al., 1983), even to the extent of having full structure refinements from intensity data collected at elevated temperatures (Dollase, 1967; Kihara, 1977, 1980). Many synthetic tridymites, however, are too fine grained for single crystal X-ray analysis and the general method of characterization has been by powder diffraction. Using the distribution and intensity relations of diffraction peaks in powder patterns, Hill and Roy (1958), Flörke (1961) and then Sato (1963a) distinguished at least two different forms of synthetic low tridymite and also suggested that some of their products consisted of a mixture of these forms, with or without cristobalite as an additional phase. Unfortunately, this method of characterization can

be rather unsatisfactory for phases with weak superlattice reflections, and, if there is a mixture of phases present, peak assignment may become difficult. In this context, transmission electron microscopy (TEM) may provide a useful adjunct to traditional X-ray methods, because it can be used to examine even very small grains and obtain diffraction information from them individually, as shown by previous studies on natural tridymite (Appleman et al., 1971) and cristobalite (Champness et al., 1971).

Since a thorough appreciation of the nature of phase transformations in any material is greatly assisted by the observation of anomalous heat capacity effects, tridymites have recently been examined by dynamical calorimetry (Shahid and Glasser, 1970; Thompson and Wennemer, 1979). Thompson and Wennemer (1979) proposed an approximate correlation between the positions of anomalous C_P effects and the transformations recognized in relatively large single crystals. They also suggested that a sample showing X-ray powder diffraction peaks appropriate for cristobalite + tridymite was an intimate intergrowth of these two phases rather than a mechanical mixture. Since cristobalite and tridymite may be represented as having a polytypic relationship to each other, there is clearly the possibility that more-or-less ordered mixed layer phases might form. The present TEM investigation was undertaken in the light of these observations and its purpose was to define the nature of superstructure types present in a number of synthetic tridymite samples, consider their transformation behavior and have a closer look at the possible mixed layer phases. Differential scanning calorimetry (DSC) results obtained from the same samples and a detailed structural interpretation of the transformations are presented elsewhere (Thompson and Wennemer, 1979; Wennemer and Thompson, in prep.).

Sample description

Silica gel or finely ground quartz powder were mixed with a variety of carbonate and tungstate fluxes. These were ground under acetone, pressed into pellets and heated in air for different times at different temperatures. Details of the high purity silica gel and of the preparation procedures for samples TR-G4, TR-G3 and CR-1 were given by Thompson and Wennemer (1979) and are summarized in Table 1. In contrast with the silica gel/carbonate mixtures, which were heated on a ceramic tablet, the quartz powder/tungstate mixtures were mixed and heated in ceramic crucibles. With the exception of T-1sa, the preparation of which has been described by Flörke and Langer (1972), all the samples were synthesized by M. Wennemer.

Powder X-ray diffraction traces over the range $2\theta = 19-37°$ (Cu$K\alpha$ radiation) for the eight tridymites and one cristobalite are shown in Figure 1. No attempt has been made to index these patterns and determine lattice parameters because the TEM observations (see below) indicate that each sample contained a mixture of low temperature superstructure types. The powder diffraction data do show, however, that the synthetic tridymites have a spread of structural states, including Sato's (1963a) M, S and MS types. In addition, both Li-Trid and K-Trid have some weak reflections at the positions of cristobalite peaks (e.g., at ~4.05Å), TR-G3 has strong cristobalite reflections and its powder pattern is quite distinct from all the other samples, both in terms of the peak

positions and intensity distribution, and CR-1 gives only sharp reflections of cristobalite.

Observations

Tridymite grains were ground under alcohol and deposited onto thin carbon films supported by copper grids. They were examined in an AEI EM6G electron microscope operating at 100 kV. The crushed fragments, typically less than a few μm in size, suffered radiation damage in the electron beam; after ~1 minute exposure they developed a speckled texture and the diffraction patterns became increasingly diffuse (see below). Using a defocussed beam, however, it was possible to photograph microstructures and diffraction patterns before degradation became a serious problem. At the necessary low levels of illumination, and because of the need for rapid recording of the diffraction patterns, careful tilting to produce perfect reciprocal lattice orientations was not feasible, and the orientation of the grain fragments had to be accepted as they were found. Although a large number of grains were examined, it was also difficult to avoid the tendency to record, preferentially, diffraction patterns with small spacings and grains with distinct microstructures. No attempt has been made, therefore, to estimate the proportions of grains in each sample showing specific features.

A further limitation of the TEM observations is that, in general, reciprocal lattice dimensions cannot be determined accurately from electron diffraction patterns. Thus we have been unable to distinguish between hexagonal, orthorhombic and monoclinic (with β near 90°) lattices that have closely related unit cell dimensions. We use the terms pseudohexagonal and pseudo-orthorhombic in our descriptions of the superlattice types to signify this uncertainty, and present only approximate lattice parameters. The terminology used for describing tridymite superstructures is also rather involved and differs among authors (see Nukui et al., 1978; Nukui and Nakazawa, 1980). All our diffraction patterns have been indexed with respect to the high temperature, hexagonal cell ($a_H \approx 5.0$Å, $c_H \approx 8.2$Å) and the superstructures are described using conventional superlattice notation. We have then tried to correlate these observations with some of the structures described elsewhere in the literature.

Perhaps the single most important observation was that each sample appeared to be inhomogeneous, consisting of a mixture of different types of low tridymite. A summary description of each sample is given in Table 1.

Superstructures

Hexagonal sublattice reflections ($a_H \approx 5.0$Å, $c_H \approx 8.2$Å) could be identified easily in electron diffraction patterns by their relatively high intensities. At least two distinct superlattices were distinguished. A common superlattice in samples T-1sa, Li-Trid and Na-Trid has reflections along $\langle 110 \rangle^*$ indicating a tripling of the d_{110} spacings and reflections along c^* that indicate a doubling of d_{001} (Fig. 2a,b) (all Miller indices are given in terms of the hexagonal sublattice). This superlattice can be described using a primitive, pseudohexagonal unit cell with $a \approx 8.7$Å and $c \approx 16.4$Å, i.e. $a = \sqrt{3}a_H$, $c = 2c_H$. This will be referred to as the $\sqrt{3}a_H \times 2c_H$ superlattice. Many orientations were indexed but the most obvious section contains c^* and $[110]^*$ (Fig. 2b). Diffraction patterns taken with the electron beam parallel to the c-axis were not found so commonly but appeared to be consistent with the proposed unit cell (Fig.

Table 1. Summary of tridymite synthesis methods, X-ray powder diffraction characteristics and TEM observations. Tentative assignments to the S, M and MS tridymite types of Sato (1963a) have been made on the basis of X-ray powder patterns (Fig. 1), only to illustrate the wide range of structural states represented by these samples. A cross signifies that a feature was observed, a dash that it was not, and a question mark that it was suspected but not positively identified. See Thompson and Wennemer (1979) for a description of the synthesis procedure for TR-G4, TR-G3, CR-1 and Flörke and Langer (1972) and T-1sa.

Sample name	Starting material	Heat treatment	Product (X-ray powder diffraction)	$\sqrt{3}a_H \times 2c_H$ superlattice	$2\sqrt{3}a_H \times 2a_H \times nc_H$ superlattice	c repeat (multiple of 8.2Å)	cristobalite
T-1sa	2:1, silica gel: Na_2WO_4	72 hrs 1400°C, cleaned, then 1 day 1400°C	S tridymite	X	X	x3,4,5,6	—
TRIII	silica gel + 1 mol% K_2CO_3	161 hrs, 1200°C	S tridymite	—	X	severe disorder	?
TRIV	silica gel + 1 mol% K_2CO_3	112 hrs, 1200°C	S tridymite	X (only one grain obs.)	X	severe disorder	X
TR-G3	silica gel + 1 mol% Na_2CO_3	overnight 750°C, 20 hrs 800°C, 15 hrs 800°C, 20 hrs 900°C, 20 hrs 1000°C	Tridymite does not fit M, S or MS. Strong cristobalite reflections.	—	X	severe disorder	X
TR-G4	silica gel + 1 mol% K_2CO_3	overnight 750°C, 20 hrs 800°C, reground, 15 hrs 800°C, 20 hrs 900°C, 20 hrs 1000°C	S tridymite	X (only one grain obs.)	X	x5, and many grains with severe disorder	—
Li-Trid	1:1 fine quartz powder: Li_2WO_4	87 hrs 1100°C, cleaned	M tridymite some cristobalite reflections	X	X	one case of a multiple c-repeat	—
Na-Trid	1:1 fine quartz powder: Na_2WO_4	192 hrs 1100°C, cleaned	MS tridymite	X	X	x4,5, some (001) stacking faults	?
K-Trid	1:1 fine quartz powder: K_2WO_4	22 days 1100°C, cleaned	M tridymite, some cristobalite reflections	X (only one grain obs.)	X	generally disordered	—
CR-1	silica gel	20 hrs 1500°C	cristobalite	—	—	—	X

2a). Twinning was not obviously present and the reflections were almost invariably sharp. Only one diffraction pattern (from a grain of K-Trid) showed signs of streaking along **c***.

A second superlattice had extra reflections along **a*** directions, representing a doubling of the d_{100} spacings of the sublattice (Fig. 2c). This can be described either with a primitive, pseudohexagonal unit cell having $a \approx 9.9$Å ($= 2a_H$), $c \approx n8.2$Å ($= nc_H$), or with a C-face centered pseudoorthorhombic cell having $a \approx 17$Å ($= 2\sqrt{3}a_H$), $b \approx 9.9$Å ($= 2a_H$), $c \approx n8.2$Å ($= nc_H$); the c dimensions were either some multiple (n) of 8.2Å, where observed values of n were 3, 4, 5, 6, or could not be specified because of strong streaking along **c***. There was typically some **c*** streaking even where multiple c-repeat reflections were present (Fig. 2d). This superlattice will be referred to as the $2\sqrt{3}a_H \times 2a_H \times nc_H$ type.

In quite a number of cases, particularly for grains from TRIV, TRIII, TR-G4 and TR-G3, the diffraction patterns

taken with the electron beam parallel to the **c**-axis resembled the $2\sqrt{3}a_H \times 2a_H \times nc_H$ types but with large distortions from orthorhombic cell parameters, having $a \approx 16.6$–17.6Å, $b \approx 8.3$–9.5Å and $\gamma \approx 81$–88°. Distortions of such magnitude are too great to be due entirely to some artefact of the electron microscope (astigmatism, misalignment, etc.) and could indicate the existence of another superstructure type. These particular samples, however, typically showed severe streaking along **c***, connecting the principal reflections, and the apparent distortions therefore might result simply from these streaks cutting the Ewald sphere in misoriented crystals.

Cristobalite grains were positively identified in TRIV and TR-G3 from their diffraction patterns and a characteristic cross-hatched twinning texture (Fig. 3), which has also been described by Champness et al. (1971). A sample of almost pure cristobalite (CR-1) was examined in the electron microscope to be sure of this identification.

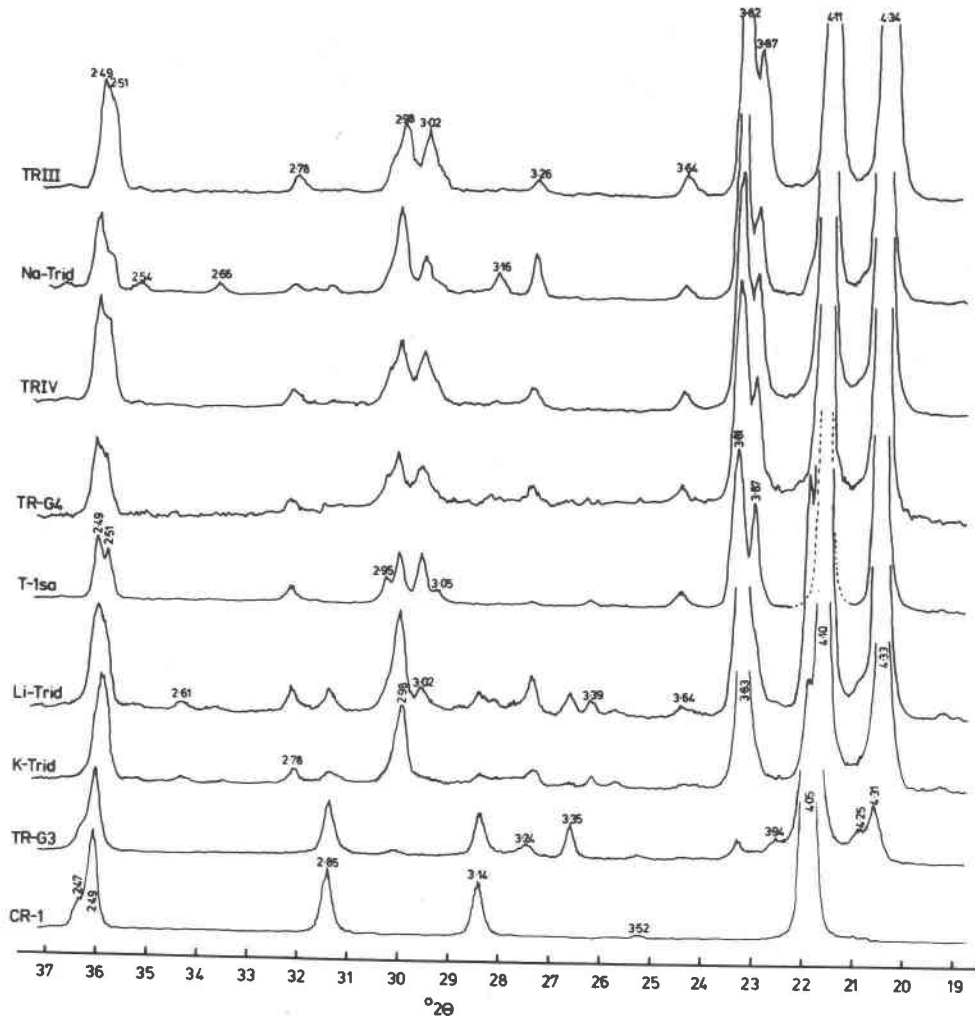A number of grains, particularly in specimens TRIII and

Fig. 1. X-ray powder diffractometer traces for $2\theta = 19-37°$ (CuK$_\alpha$ radiation) for the synthetic tridymites and cristobalite (CR-1) examined by TEM. Approximate d spacings in Å are given for some of the peaks. The 4.10Å peak of T-1sa is shown by a dashed line simply to avoid confusion with the 4.05Å + 4.10Å peak of the Li-Trid trace. All the peaks that have been truncated are single; thus the 4.05Å peak of TR-G3 shows no sign of an additional 4.11Å component. Note that there are considerable variations among the samples, indicating a range of structural states. For the purposes of easy comparison with other synthetic tridymite powders, the samples have been tentatively ascribed to Sato's (1963a) scheme as: type M (relatively strong reflection at $d \sim 3.25$Å, no doublets)—Li-Trid and K-Trid; type S (reflection at $d \sim 3.25$Å is weak, doublets at $d \sim 3.85$Å, 3.00Å, 2.50Å)—TRIII, TRIV, TR-G4, T-1sa; type MS (relatively strong reflection at $d \sim 3.25$Å, +doublets)—Na-Trid.

TRIV, had diffraction patterns that could not be indexed easily either on the basis of the above tridymite super-structures or on the basis of a cristobalite cell (Fig. 4). These typically contained doubling type superlattice reflec-tions, abundant streaking (Fig. 4e) and, in some cases, evi-dence of twinning (Fig. 4a–d). One reciprocal lattice dimen-sion, however, could usually be fit to either tridymite or cristobalite.

A few grains of tridymite from the Steinbach meteorite were crushed and examined for comparison with the syn-thetic samples. Again the small crystal fragments seemed to show more than one superstructure type. Many grains gave diffraction patterns that could be indexed using the mono-

clinic (Cc) cell given by Kato and Nukui (1976)[1] (Fig. 5a,c,d) and many using the $\sqrt{3}a_H \times 2c_H$ superlattice (Fig.

[1] Two unit cells have been used for the monoclinic Cc struc-ture: $a = 18.5$Å, $b = 5.0$Å, $c = 25.8$Å, $\beta = 118°$ (Hoffmann, 1967; Kato and Nukui, 1976; Nukui et al., 1978, 1980) and $a = 18.5$Å, $b = 5.0$Å, $c = 23.8$Å, $\beta = 106°$ (Dollase and Buerger, 1966; Dollase et al., 1971; Dollase and Baur, 1976). Each cell has the same b^* and c^* directions but the a^* direction has been chosen differently. With reference to the hexagonal high temperature structure: for the cell with $\beta = 118°$, $a^*_{Cc} \parallel c^*_H$, $b^*_{Cc} \parallel [\bar{1}20]^*_H$, $c^*_{Cc} \parallel [101]^*_H$, and for the cell with $\beta = 106°$, $a^*_{Cc} \parallel [10\bar{2}]^*_H$, $b^*_{Cc} \parallel [\bar{1}20]^*_H$, $c^*_{Cc} \parallel [101]^*_H$. The Cc structure corresponds to the hexagonal high temperature structure with $d_{101_H} \times 6$.
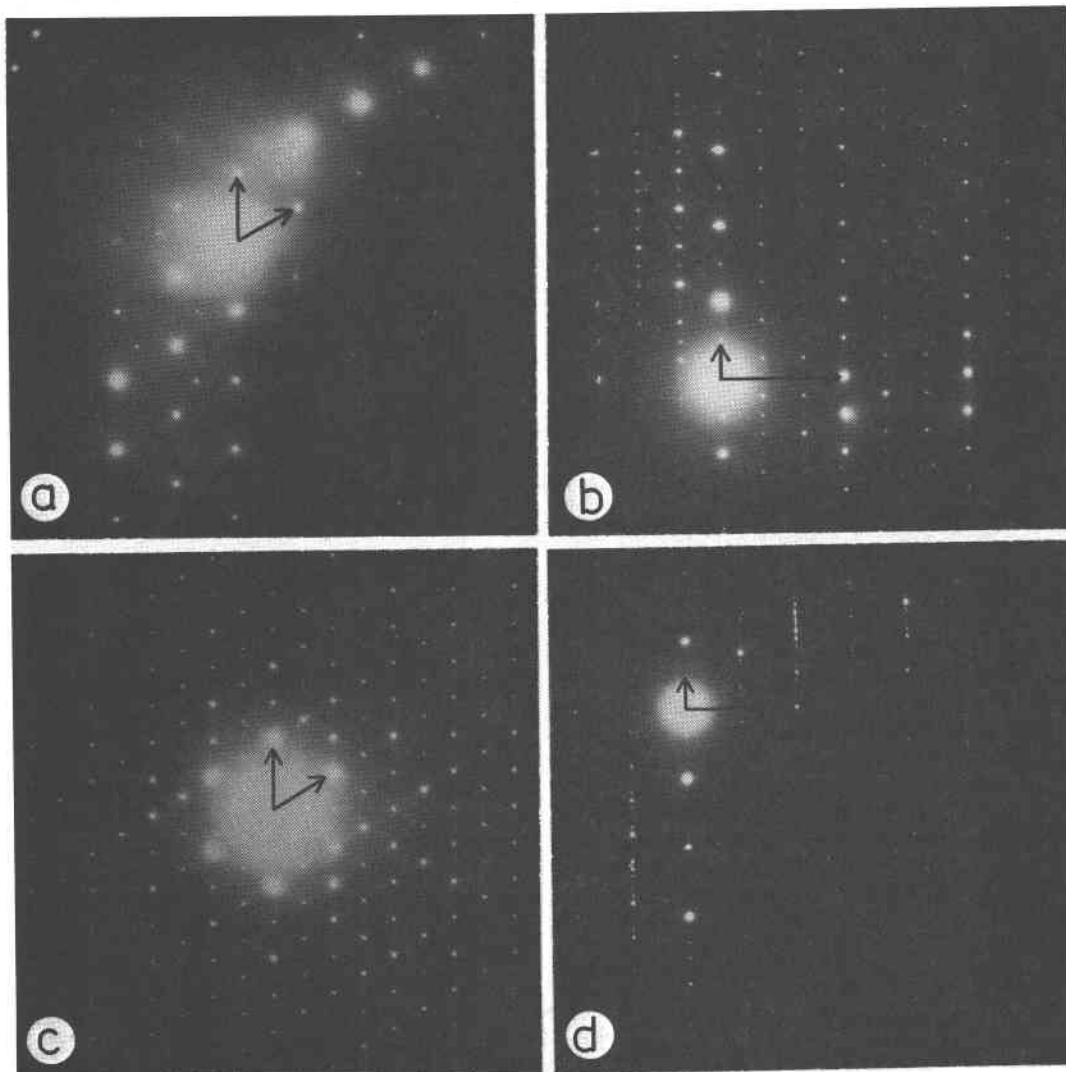
Fig. 2. Selected-area electron diffraction patterns from grains of synthetic tridymite showing additional reflections consistent with $d_{110} \times 3$, $d_{001} \times 2$ ($= \sqrt{3}a_H \times 2c_H$ pseudohexagonal superstructure) (a,b) and $d_{100} \times 2$, $d_{001} \times n$ ($= 2\sqrt{3}a_H \times 2a_H \times nc_H$ pseudoorthorhombic superstructure) (c,d). Indexing is based on the high temperature, hexagonal subcell. (a) (001) section of the $\sqrt{3}a_H \times 2c_H$ superlattice. Note tripling reflections along $\langle 110 \rangle^*$. T-1sa. Arrows are along $[100]^*$ and $[010]^*$. (b) c^* (vertical)-$[110]^*$ (horizontal) section of the $\sqrt{3}a_H \times 2c_H$ superlattice. Note tripling reflections along $[110]^*$ and doubling along c^*. T-1sa. (c) (001) section of the $2\sqrt{3}a_H \times 2a_H \times nc_H$ superlattice. Note doubling reflections along $\langle 100 \rangle^*$. TR-G4. Arrows are along $[100]^*$ and $[010]^*$. (d) c^* (vertical)-$[110]^*$ (horizontal) section of the $2\sqrt{3}a_H \times 2a_H \times nc_H$ superlattice. Note doubling along $[110]^*$ and multiple repeat along c^*. In this case the c^* repeat is close to $n = 5$ but may actually be incommensurate; there is also some streaking. T-1sa.

5b,e,f). They were notably free of microstructure.

Beam heating experiments

It was possible to induce a high/low transformation in the tridymites by beam heating. Grains were examined initially using a broadly defocussed beam. By carefully focussing the beam the grains could be heated and then recooled simply by defocussing again. This technique has been used extensively for the study of phase transformations in sulphides (Putnis, 1976). Grains with the $2\sqrt{3}a_H \times 2a_H \times nc_H$ superlattice could be reversibly transformed; at some relatively high temperature the superlattice reflections disap-

peared, leaving the $a_H \approx 5.0$Å, $c_H \approx 8.2$Å sublattice. On cooling, the $2\sqrt{3}a_H \times 2a_H \times nc_H$ superlattice reflections reappeared (Fig. 6a–c). The heating and cooling cycle could be followed a number of times until beam degradation set in. At this point the superlattice reflections failed to reappear and very diffuse streaking between the sublattice reflections developed. In some cases the intensity distribution in the recooled superstructure was not identical to the initial distribution, suggesting that the transformation is not necessarily perfectly reversible; for example, the multiplicity (n) of the c repeat might change.

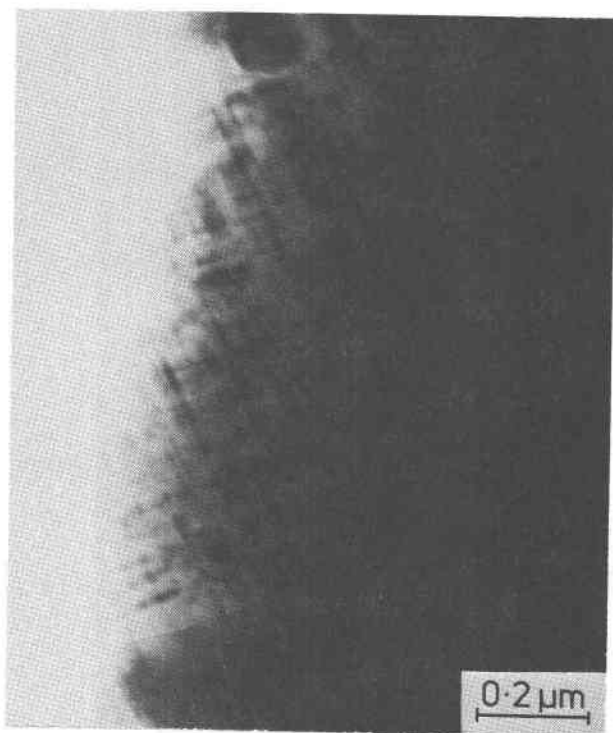The $\sqrt{3}a_H \times 2c_H$ superlattice could also be heated and

Fig. 3. Typical cross-hatched twinning texture in cristobalite (CR-1). Similar textures were observed in grains from TRIV and TR-G3. Bright field image.

transformed to the high temperature sublattice. However, on cooling, it invariably transformed to the $2\sqrt{3}a_H \times 2a_H \times nc_H$ superstructure, sometimes with a non-rational multiple c-repeat (Fig. 6d–f). This could then be reversibly transformed in the same way as grains that started with the $2\sqrt{3}a \times 2a_H \times nc_H$ superlattice.

Grains whose diffraction patterns could not be indexed on either of the two superlattice types but which showed doubling reflections could also be transformed. The doubling reflections disappeared on heating and returned on cooling. Some of the streaked intensity in the initial diffraction patterns remained throughout these heating experiments, indicating that at least part of the disorder is inherent in the substructure and is not due to some high/low transformation.

(001) stacking disorder

Tridymite grains in TRIII, TRIV, TR-G3 and TR-G4 had severe (001) stacking disorder, as shown by streaking along c^* in diffraction patterns and abundant stacking faults in bright field images (Fig. 7a). Grains in K-Trid were generally disordered, but in the other specimens far fewer stacking faults were observed.

In some grains there appeared to be well ordered regions a few hundred ångströms wide intermixed with regions of very closely spaced stacking faults (Fig. 7b). These grains may be intimate intergrowths of more-or-less ordered

tridymite and cristobalite. An attempt to image (001) lattice fringes in a JEM 100C electron microscope proved fruitless because of a high rate of beam damage to the specimens in this instrument.

The severely disordered grains showed superlattice reflections of the $2\sqrt{3}a_H \times 2a_H \times nc_H$ type and these could be removed reversibly by beam heating. Similarly, the grains with diffraction patterns that could not be indexed readily as cristobalite or tridymite superstructures, and that also had some stacking disorder, showed the doubling behavior. It appears that stacking disorder is associated with doubling type superstructures whereas well crystallized, ordered tridymites tend to have the $\sqrt{3}a_H \times 2c_H$ type of superstructure.

Electron irradiation damage

Figure 8 illustrates the effects of radiation damage on the tridymite structure. The mottled texture that developed in individual grains exposed to the electron beam was accompanied by changes in their diffraction patterns. With exposure to the beam, first the superlattice reflections progressively fade away, leaving some diffuse streaking (Fig. 8a–d). With further exposure even some of the sublattice reflections fade, leaving a structure with a 4Å c repeat (Fig. 8e). The electron beam is responsible for reorganizing Si–O bonds by the process of radiolysis (Hobbs, 1975, 1976). Electrons in the solid are excited by inelastic scattering of the incident electrons and this causes bonding instabilities. Progressive disordering of the atomic displacements that combine to give the low temperature superlattice causes the extra reflections to fade and become diffuse. Only a limited amount of this kind of disruption is needed to cause the grains to be stranded with the sublattice structure during the high⇌low beam heating experiments. The final 4Å repeat (Fig. 8e) may come from single layers of SiO_4 tetrahedra, showing that the ABABA.... stacking sequence of tridymite is effectively reduced to a disordered sequence with an average one layer repeat. Dollase et al. (1971) reported the appearance of diffuse intensity in X-ray diffraction patterns after long exposure of single crystals to X-rays, and this may be equivalent to the effect of electron radiation damage.

Discussion

It should be emphasized at this point that the TEM observations have two shortcomings. First, since the samples appeared to contain a mixture of low temperature forms and each electron diffraction pattern gives information in only two dimensions, the task of reconstructing the complete reciprocal lattice geometry of each superstructure was not straightforward. Proper indexing of some of the possible mixed layer phases was not achieved. Second, the beam heating technique produces temperatures that are unknown and are not well controlled. These difficulties do not, however, preclude a discussion of some of the more general issues raised by the observations.

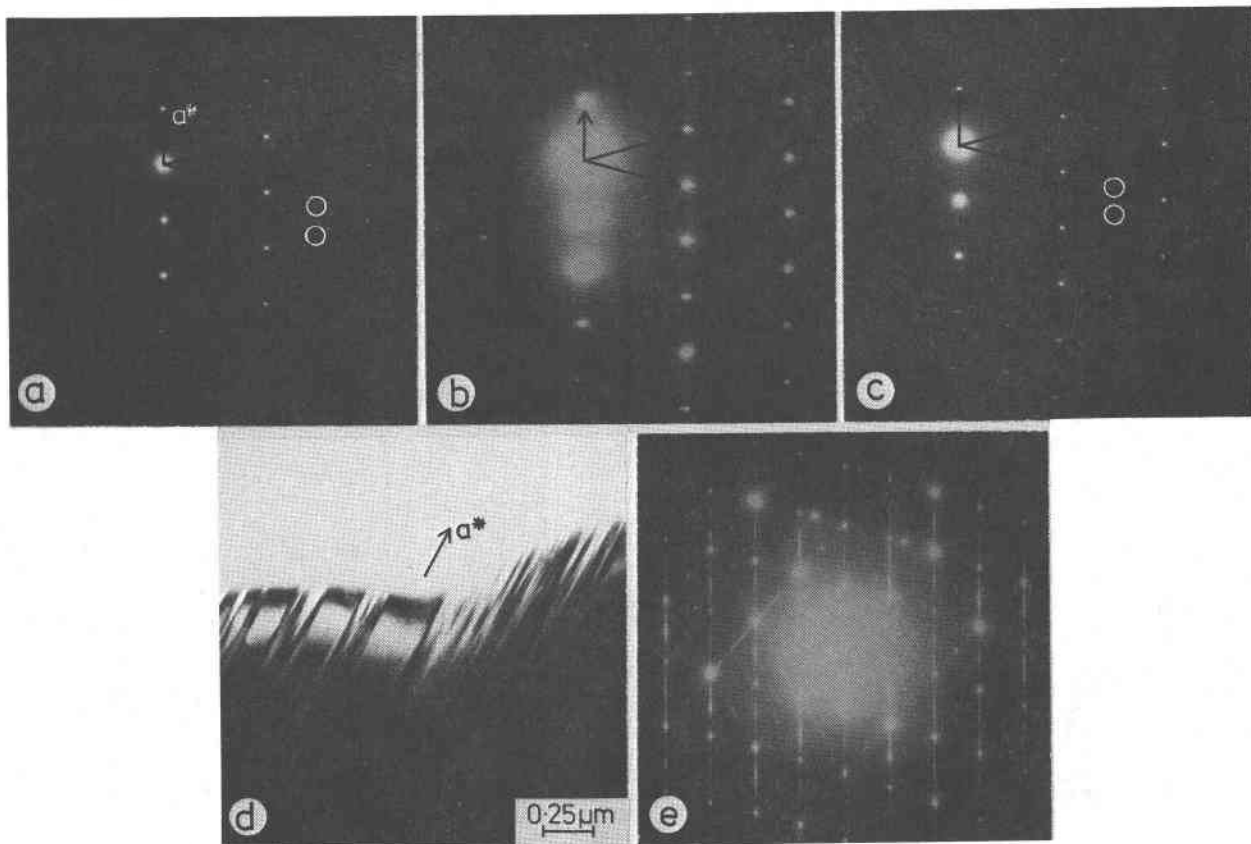Flörke (1955), Sato (1963a) and Hill and Roy (1958) have

Fig. 4. (a–c) Selected-area electron diffraction patterns from grain of TRIII shown in (d). (a) Initial diffraction pattern; **a*** vertical, [013]* shown in possible twin related orientations. Typical doubling reflections are circled. (b) Same grain as (a) but with focussed, beam heated conditions; doubling reflections now absent. (c) Same grain as (b) after cooling. Note the reappearance of doubling reflections (e.g. circled). (d) Bright field image of grain from which (a)-(c) were taken. The stacking faults visible in this micrograph were not affected by the beam heating transformations. The spotty texture is due to radiation damage. (e) Typical diffraction pattern from a disordered grain of TRIV, with multiple reflections and streaking.

suggested that some synthetic tridymite samples contain more than one phase. This supposition was supported by Shahid and Glasser (1970), who observed tridymite grains with different optical properties in some of their run products, and is confirmed in the present study. We have found two main types of well defined superstructures, the $\sqrt{3}a_H \times 2c_H$ and $2\sqrt{3}a_H \times 2a_H \times nc_H$ types. In the latter group the value of n can vary from grain to grain in a single sample (Table 1). In addition, a third general group of structures had severe (001) stacking disorder.

Our $\sqrt{3}a_H \times 2c_H$ superstructure appears to correspond closely to the MX-1 structure described by Hoffmann et al. (1983), who used a C-face centered unit cell with $a = a_H$, $b = \sqrt{3}a_H$, $c = c_H$, $\beta = 91.5°$ and incommensurate superlattice reflections at approximately $h \pm n2/3$, k, $l \mp n1/2$ (n = 1,2). In all our diffraction patterns, however, the $\sqrt{3}a_H \times 2c_H$ superstructure seems to be commensurate. Hoffmann et al. (1983) suggested that MX-1 is essentially the same as S1 of Sato (1964), and the cell dimensions they give are almost identical to those given by Flörke and Langer

(1972) for T-1sa. They also reported that, on heating, MX-1 grains transform to pseudo-orthorhombic (PO in the terminology of Nukui and Nakazawa, 1980) structures, equivalent to the S1⇌S2 transformation of Sato (1964). Our $\sqrt{3}a_H \times 2c_H$ structure also transforms to a PO structure $(2\sqrt{3}a_H \times 2a_H \times nc_H)$ but the transformation is irreversible and occurs via the high temperature $a_H \times c_H$ structure.

Our $2\sqrt{3}a_H \times 2a_H \times nc_H$ superstructures correspond to the pseudo-orthorhombic (PO) superstructures of Nukui and Nakazawa (1980) and are also consistent with the M and S types of Sato (1963a,b; 1964). Natural terrestrial samples have essentially the same superstructure, usually with n = 5 or 10 (PO-5, PO-10 in the terminology of Nukui and Nakazawa, 1980) (Buerger and Lukesh, 1942; Tagai and Sadanaga, 1972; Gardner and Appleman, 1974; Konnert and Appleman, 1978; Kawai et al., 1978; Nukui et al., 1980). Nukui and Nakazawa (1980) have summarized the full range of values of n reported previously; these are n = 1, 1.5, 2, 5, 6 and 10, to which may now be added n = 3 and n = 4 (Table 1).
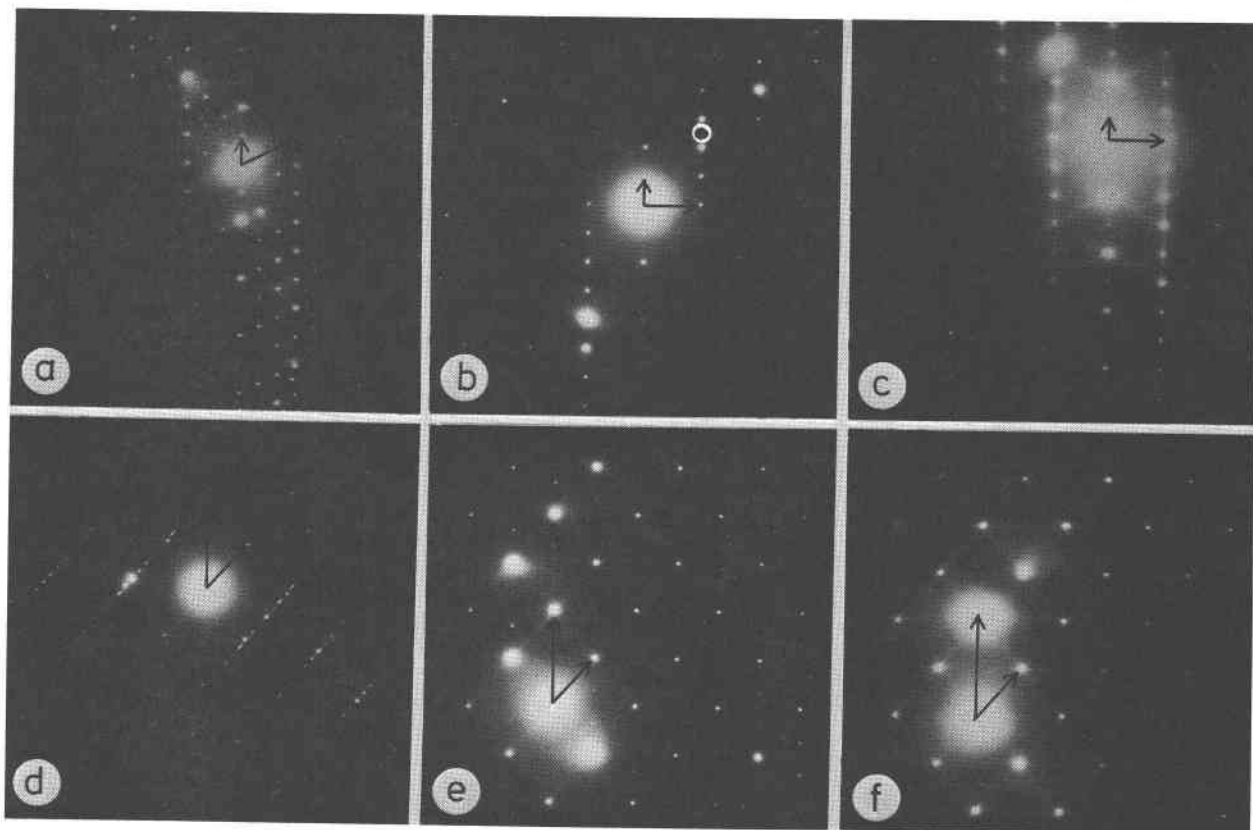
Fig. 5. Selected-area electron diffraction patterns from grains of tridymite from the Steinbach meteorite. (a) $a_{Cc}^* - c_{Cc}^*$ section of Cc tridymite. This diffraction pattern has been indexed on the Cc lattice of Kato and Nukui (1976) and the arrows are parallel to a_{Cc}^* (vertical) and c_{Cc}^*, ending at the 200 and 006 reflections respectively. l = odd reflections are absent due to the c-glide and h = odd are absent due to the C-face centering condition (in $h0l$) (see footnote 1 for orientation relationships between the monoclinic Cc lattice and the high temperature hexagonal lattice). (b) The same orientation as (a) but from a grain with the $\sqrt{3}a_H \times 2c_H$ superlattice. Arrows indicate principal directions in the hexagonal sublattice; c_H^* vertical, a_H^* horizontal. Note doubling reflections along c^* (e.g., circled). (c) From same grain as (a) after prolonged beam exposure. Arrows as in (b). Superlattice reflections now absent. (d) Cc tridymite. Based on the hexagonal ($a_H = 5$Å, $c_H = 8.2$Å) sublattice: $[110]_H^*$ vertical, $[101]_H^*$ indicated by second arrow which is also c_{Cc}^* (i.e., c^* of the Cc superstructure) with multiple ($\times 6$) superlattice reflections (see footnote 1). (e) $\sqrt{3}a_H \times 2c_H$ superlattice. Same orientation as (d) showing superlattice reflections ($\times 3$) along $[110]_H^*$. (f) From same grain as (e) after prolonged exposure to the electron beam.

Monoclinic Cc tridymite (=MC structure of Nukui et al., 1978, Nukui and Nakazawa, 1980) was not found in any of the synthetic samples. Its apparent absence cannot have been due solely to a problem of identification since it could be recognized in the Steinbach meteorite sample. The fine-grained synthetic tridymites therefore appear to be quite different from most, relatively large, natural and synthetic single crystals. Hoffmann et al. (1983) reported that MX-1 tridymite, which seems to be the same as our $\sqrt{3}a_H \times 2c_H$ superstructure, can be produced from Cc tridymite by non-hydrostatic pressure during grinding. We are unable to state unequivocally, therefore, that Cc grains were entirely absent from the synthetic tridymites prior to their being crushed for TEM study.

Given these detailed observations of a diversity of superstructures and microstructures in individual tridymite sam-

ples, it is not surprising that the transformation behavior of synthetic powders does not correlate exactly with that observed in single crystals (Nukui et al., 1978; Thompson and Wennemer, 1979). Even sample T-1sa, which Flörke and Langer (1972) described as a well ordered low tridymite, shows pressure dependent effects for the displacive transformations that do not appear to be consistent with the unit cell volume data of Nukui et al. (1978) for single crystals (Cohen and Klement, 1980). Variations between tridymites have in the past been attributed at least partly to differing impurity contents and crystallinity (Buerger and Lukesh, 1942; Flörke, 1955, 1961; Eitel, 1957; Sato, 1963a; Sosman, 1965; Flörke and Müller-Vonmoos, 1971; Flörke and Langer, 1972; Schneider and Flörke, 1982), but grain size may also be important. Since the high/low transformations are thought to be displacive in character (Buerger,
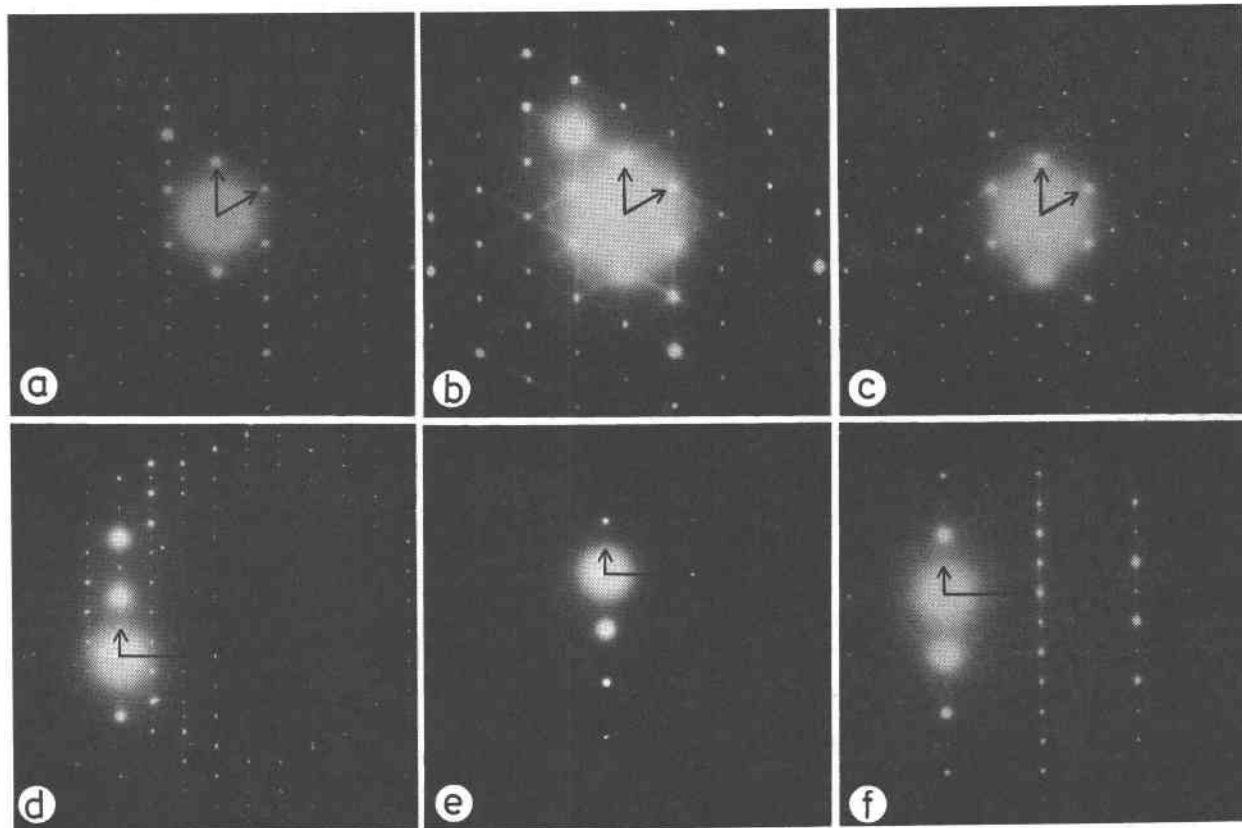
Fig. 6. Selected-area electron diffraction patterns obtained during beam heating experiments. (a)–(c) and (d)–(f) are representative of two separate sequences. (a) (001) section of the $2\sqrt{3}a_H \times 2a_H \times nc_H$ superlattice, initial state. TRIV. (b) High temperature sublattice. Same grain as (a) but with highly focussed electron beam. Doubling reflections now absent. Diffuse intensity may be due to thermal diffuse scattering. (c) Same grain as (a) and (b), but with electron beam defocussed. Doubling reflections have reappeared but not with the exact initial intensity distribution. (d) $c^* - [110]^*$ section of the $\sqrt{3}a_H \times 2c_H$ superlattice. Defocussed beam, initial state. c^* vertical, $[110]^*$ horizontal. T-1sa. (e) High temperature form (focussed beam); superlattice reflections absent. This diffraction pattern was not obtained from the same grain as (d) but is typical of the low–high–low sequence induced by beam heating. (f) Low temperature form, after defocussing beam. Same grain as (d). Note that $[110]^*$ is now doubled and c^* shows a multiple repeat.

1951) strain effects probably contribute to the stability and kinetic accessibility of the most favored structures. Clearly the strain distribution across a tiny flake of crystals, less than a few μm across and only hundreds of ångströms thick, may be different from that in a much larger crystal. It is possible, therefore, that the superstructures we have found in the synthetic powders are either the products of grinding or are merely the low temperature modifications most favored by small crystals. The presence of $\sqrt{3}a_H \times 2c_H$ grains in the Steinbach sample is consistent with this suggestion if they form from the large Cc crystals on being crushed into smaller fragments. Our failure to observe intermediate structures in the beam heating experiments may further indicate different behavior for very small grains but could also be due to the lack of precise temperature control.

As has been discussed by many authors (Flörke, 1955, 1967; Eitel, 1957; Sosman, 1965; Shahid and Glasser, 1970;

Flörke and Müller-Vonmoos, 1971) the transformation behavior of individual tridymite grains also appears to depend on their degree of (001) stacking disorder. Our observations are that well ordered grains may have the $\sqrt{3}a_H \times 2c_H$ superstructure, in contrast with the disordered grains, which have $2\sqrt{3}a_H \times 2a_H \times nc_H$ type superstructures. Again, the strain distribution during structural collapse is bound to be affected by the presence of (001) stacking faults though variations in the multiplicity of the c-repeat did not correlate obviously with the presence of stacking faults. Grains that appeared to be intimate intergrowths of more-or-less ordered regions seemed to have their own diffraction characteristics, distinct from either tridymite or cristobalite. The problematical diffraction patterns from such grains could be due to a compromise low-temperature distorted structure. Specimen TR-G3, which contained material of this type, was used by Thompson and Wennemer (1979) for differential scanning calorimetry.
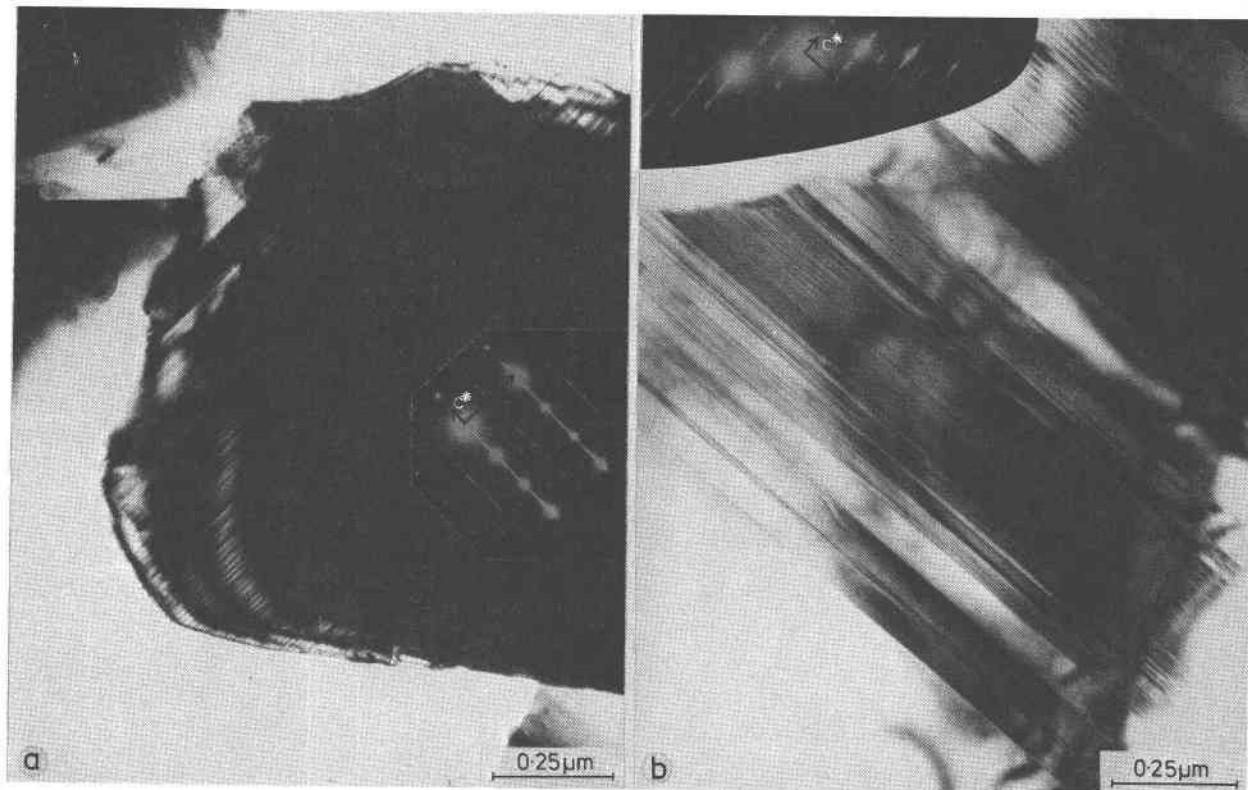
Fig. 7. Mixed layer (?) phases. (a) Bright field image of a grain from TRIV with abundant (001) stacking faults. Inset is the diffraction pattern ($c^* − [110]^*$) from the same grain. (b) Bright field image of a grain from TR-G3 showing ordered regions interspersed with regions of abundant stacking faults. Inset is the diffraction pattern from this grain ($a^*–c^*$). Note the streaking along c^* and the doubling reflections along a^*.

They showed that, in spite of X-ray and infra-red properties appropriate for a mechanical mixture of tridymite and cristobalite, the excess C_p effects were distinct from either. The DSC and TEM observations are thus consistent in implying the presence of mixed-layer phases that have their own distinctive transformation behavior.

With regard to the influence of impurity atoms, the proportions of Na^+, K^+, and Li^+ that can enter the tridymite structure remain uncertain. We have found, however, that samples of T-1sa, Li-Trid and Na-Trid, which were prepared with Na and Li tungstate fluxes (see Table 1), were more ordered than the samples prepared with K_2WO_4 or Na_2CO_3/K_2CO_3 fluxes. Whether the $\sqrt{3}a_H \times 2c_H$ superstructure results from better crystallinity due to more efficient flux action, or from the incorporation of small amounts of Na^+ and Li^+ ions, is not clear. It is notable that Shahid and Glasser (1970) also found that samples prepared with a K_2WO_4 flux have a high degree of stacking disorder.

A variety of low temperature superstructures has now been recognized in tridymites, including the monoclinic Cc form, both as natural and synthetic crystals (Fleming and Lynton, 1960; Dollase and Buerger, 1966; Hoffmann, 1967; Dollase, 1967; Dollase et al., 1971; Dollase and Baur, 1976;

Kato and Nukui, 1976; Kihara, 1977; Tagai et al., 1977; Kawai et al., 1978); pseudo-orthorhombic types with $a \approx 2\sqrt{3}a_H$, $b \approx 2a_H$ and with c disordered or some multiple (n) of 8.2Å, n = 1, 1.5, 2, 3, 4, 5, 6, 10 (Buerger and Lukesh, 1942; Sato, 1963a, b, 1964; Hoffman and Laves, 1964; Dollase et al., 1971; Kawai et al., 1978; Nukui et al., 1980; Nukui and Nakazawa, 1980; Schneider and Flörke, 1982; this study); and a pseudohexagonal form with $a \approx 8.7$Å, $c \approx 16.4$Å (Hoffmann et al., 1983; this study). Konnert and Appleman (1978) have refined the pseudo-orthorhombic structure with n = 10 under $F1$ (triclinic) symmetry. It is even possible to find two different forms coexisting in nature (e.g. Kawai et al., 1978). The complex series of transformations that occurs during heating is rarely reproducible in different samples (Kihara, 1977; Nukui et al., 1978) and is frequently irreversible (Buerger and Lukesh, 1942; Kawai et al., 1978; Thompson and Wennemer, 1979; Wennemer and Thompson, in preparation; this study). Such an association of properties indicates a very delicate energetic and/or kinetic balance between possible distortions of the tridymite framework, and is typical of alternative transformation behavior, in which an equilibrium state is not achieved. Metastable modifications that lower the energy and are kinetically favored develop instead, and
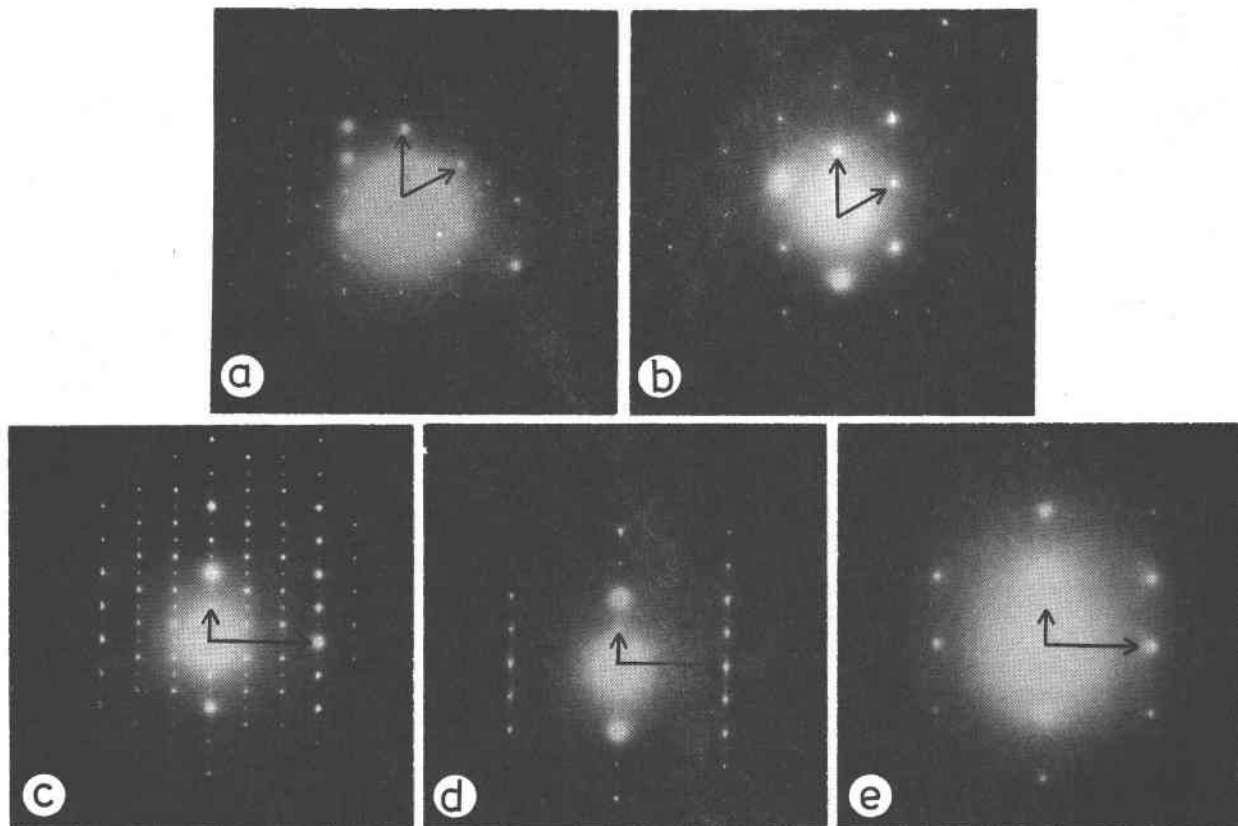
Fig. 8. Effects of beam degradation. Prolonged exposure to the electron beam causes the disappearance of superlattice reflections and the development of diffuse scattered intensity. (a) (001) section of the $2\sqrt{3}a_H \times 2a_H \times nc_H$ superlattice. TR-G3. Arrows are along $[100]^*$ and $[010]^*$ of the hexagonal sublattice. (b) Same grain as (a) after exposure to the electron beam for 1–2 minutes. (c) Initial pattern from a $\sqrt{3}a_H \times 2c_H$ grain; c^* vertical and $[110]^*$ horizontal. Steinbach tridymite. (d) Same grain as (c) after exposure; superlattice reflections now absent. (e) Same grain as (c) after further exposure. Some of the sublattice reflections have now faded, leaving a 4Å (one layer) repeat along c^*.

the delicate balance is such as to be influenced readily by any feature, such as heat treatment, grinding, impurity content, defect concentration and associated flux or fluid composition, which can cause one particular distortion to be more accessible than a slightly different one. Under these circumstances, the understanding of transformation behavior in both synthetic and natural specimens requires very thorough sample characterization, and the methods outlined here may provide a useful means towards this end. Closely analogous issues may arise in the study of transformations in sub-potassic nephelines, which have a stuffed tridymite type of structure (Henderson and Roux, 1977; Henderson and Thompson, 1980).

References

Appleman, D. E., Nissen, H.-U., Stewart, D. B., Clark, J. R., Dowty, Eric, and Huebner, J. S. (1971) Studies of lunar plagioclases, tridymite, and cristobalite. Proceedings of the Second Lunar Science Conference, 1, 117–133.

Buerger, M. J. (1951) Crystallographic aspects of phase transformations. In R. Smoluchowski, J. E. Mayer and W. A. Weyl, Eds., Phase Transformations in Solids, p. 183–211. Wiley, New York.

Buerger, M. J. and Lukesh, Joseph (1942) The tridymite problem. Science, 95, 20–21.

Champness, P. E., Dunham, A. C., Gibb, F. G. F., Giles, H. N., MacKenzie, W. S., Stumpfl, E. F., and Zussman, Jack (1971) Mineralogy and petrology of some Apollo 12 lunar samples. Proceedings of the Second Lunar Science Conference, 1, 359–376.

Cohen, L. H. and Klement, William, Jr. (1980) Tridymite: effect of

hydrostatic pressure to 6 kbar on temperatures of two rapidly reversible transitions. Contributions to Mineralogy and Petrology, 71, 401–405.

Dollase, W. A. (1967) The crystal structure at 220°C of orthorhombic high tridymite from the Steinbach meteorite. Acta Crystallographica, 23, 617–623.

Dollase, W. A. and Baur, W. H. (1976) The superstructure of meteoritic low tridymite solved by computer simulation. American Mineralogist, 61, 971–978.

Dollase, W. A. and Buerger, M. J. (1966) Crystal structure of some meteoritic tridymites. Geological Society of America Abstracts with Program, 1966 Annual Meeting, 54–55.

Dollase, W. A., Cliff, R. A., and Wetherill, G. W. (1971) Note on tridymite in rock 12021. Proceedings of the Second Lunar Science Conference, 1, 141–142.

Eitel, Wilhelm (1957) Structural anomalies in tridymite and cristobalite. A review of the paper with the same title by O. W. Flörke published in Berichte der Deutschen Keramischen Gesellschaft, 32, 369–381 (1955). American Ceramic Society Bulletin, 36, 142–148.

Fenner, C. N. (1913) The stability relations of the silica minerals. American Journal of Science, 36, 331–384.

Fleming, J. E. and Lynton, H. (1960) A preliminary study of the crystal structure of low tridymite. Physics and Chemistry of Glasses, 1, 148–154.

Flörke, O. W. (1955) Strukturanomalien bei Tridymit und Cristobalit. Berichte der Deutschen Keramischen Gesellschaft, 32, 369–381.

Flörke, O. W. (1961) Die Kristallarten des SiO_2 und ihr Umwandlungsverhalten. Berichte der Deutschen Keramischen Gesellschaft, 38, 89–97.

Flörke, O. W. (1967) Die Modifikationen von SiO_2. Fortschritte der Mineralogie, 44, 181–230.

Flörke, O. W. and Langer, K. (1972) Hydrothermal recrystallization and transformation of tridymite. Contributions to Mineralogy and Petrology, 36, 221–230.

Flörke, O. W. and Müller-Vonmoos, M. (1971) Displazive Tief-Hoch-Umwandlung von Tridymit. Zeitschrift für Kristallographie, 133, 193–202.

Gardner, S. P. and Appleman, D. E. (1974) X-ray crystallography and polytypism of naturally-occurring tridymite, SiO_2. American Crystallographic Association Program and Abstracts, 2, 271.

Gibbs, R. E. (1926) The polymorphism of silicon dioxide and the structure of tridymite. Proceedings of the Royal Society of London, A113, 351–368.

Henderson, C. M. B. and Roux, J. (1977) Inversions in sub-potassic nephelines. Contributions to Mineralogy and Petrology, 61, 279–298.

Henderson, C. M. B. and Thompson, A. B. (1980) The low-temperature inversion in sub-potassic nepheline. American Mineralogist, 65, 970–980.

Hill, V. G. and Roy, Rustum (1958) Silica structure studies VI. On tridymites. Transactions of the British Ceramic Society, 57, 496–510.

Hobbs, L. W. (1975) Transmission electron microscopy of extended defects in alkali halide crystals. In M. W. Roberts and J. M. Thomas, Eds., Surface and defect properties of solids, volume 4, p. 152–250. Chemical Society, London.

Hobbs, L. W. (1976) Radiation effects in the electron microscopy of beam-sensitive inorganic solids. In J. A. Venables, Ed., Developments in electron microscopy and analysis, p. 287–292. Academic Press, London, New York, San Francisco.

Hoffmann, W. (1967) Gitterkonstanten und Raumgruppe von Tridymit bei 20°C. Naturwissenschaften, 54, 114.

Hoffmann, W. and Laves, Fritz (1964) Zur Polytypie und Polytropie von Tridymit. Naturwissenschaften, 51, 335.

Hoffmann, W., Kockmeyer, M., Löns, J., and Vach, Chr. (1983) The transformation of monoclinic low-tridymite MC to a phase with an incommensurate superstructure. Fortschritte der Mineralogie, 61, Beiheft 1, 96–98.

Kato, Katsuo and Nukui, Akihiko (1976) Die Kristallstruktur des monoklinen Tief-Tridymits. Acta Crystallographica, B32, 2486–2491.

Kawai, Kazuhide, Matsomoto, Takeo, Kihara, Kuniaki, and Sakurai, Kin-ichi (1978) The first finding of monoclinic tridymite in terrestrial volcanic rocks. Mineralogical Journal, 9, 231–235.

Kihara, Kuniaki (1977) An orthorhombic superstructure of tridymite existing between about 105 and 180°C. Zeitschrift für Kristallographie, 146, 185–203.

Kihara, Kuniaki (1978) Thermal change in unit-cell dimensions, and a hexagonal structure of tridymite. Zeitschrift für Kristallographie, 148, 237–253.

Kihara, Kuniaki (1980) On the split-atom model for hexagonal tridymite. Zeitschrift für Kristallographie, 152, 95–101.

Konnert, J. H. and Appleman, D. E. (1978) The crystal structure of low tridymite. Acta Crystallographica, B34, 391–403.

Mosesman, M. A. and Pitzer, K. S. (1941) Thermodynamic properties of the crystalline forms of silica. Journal of the American Chemical Society, 63, 2348–2356.

Nukui, Akihiko and Nakazawa, Hiromoto (1980) Polymorphism in tridymite. Kobutugaku-Zasshi (Journal of the Mineralogical Society of Japan), 14, Special Volume no. 2, 364–386.

Nukui, Akihiko, Nakazawa, Hiromoto, and Akao, Masaru (1978) Thermal changes in monoclinic tridymite. American Mineralogist, 63, 1252–1259.

Nukui, Akihiko, Yamaoka, Shinobu, and Nakazawa, Hiromoto (1980) Pressure-induced phase transitions in tridymite. American Mineralogist, 65, 1283–1286.

Putnis, Andrew (1976) Alternative transformation behaviour in sulfides: direct observations by transmission electron microscopy. Science, 193, 417–418.

Sato, Mitsuo (1963a) X-ray study of tridymite (1). On tridymite M and tridymite S. Mineralogical Journal, 4, 115–130.

Sato, Mitsuo (1963b) X-ray study of low tridymite (2). Structure of low tridymite, type M. Mineralogical Journal, 4, 131–146.

Sato, Mitsuo (1964) X-ray study of tridymite (3). Unit cell dimensions and phase transition of tridymite, type S. Mineralogical Journal, 4, 215–225.

Schneider, H., and Flörke, O. W. (1982) Microstructure, chemical composition, and structural state of tridymite. Neues Jahrbuch für Mineralogie Abhandlungen, 145, 280–290.

Shahid, K. A. and Glasser, F. P. (1970) Thermal properties of tridymite: 25°C–300°C. Journal of Thermal Analysis, 2, 181–190.

Sosman, R. B. (1965) The Phases of Silica. Rutgers University Press, New Jersey.

Tagai, Tokuhei and Sadanaga, Ryoichi (1972) Tridymite, features of its high-low transitions and structure of its 20-layer polytype. Acta Crystallographica, A28, S121.

Tagai, Tokuhei, Sadanaga, Ryoichi, Takeuchi, Yoshio, and Takeda, Hiroshi (1977) Twinning of tridymite from the Steinbach meteorite. Mineralogical Journal, 8, 382–398.

Thompson, A. B. and Wennemer, Mechthild (1979) Heat capacities and inversions in tridymite, cristobalite and tridymite-cristobalite mixed phases. American Mineralogist, 64, 1018–1026.